

General Disclaimer

One or more of the Following Statements may affect this Document

- This document has been reproduced from the best copy furnished by the organizational source. It is being released in the interest of making available as much information as possible.
- This document may contain data, which exceeds the sheet parameters. It was furnished in this condition by the organizational source and is the best copy available.
- This document may contain tone-on-tone or color graphs, charts and/or pictures, which have been reproduced in black and white.
- This document is paginated as submitted by the original source.
- Portions of this document are not fully legible due to the historical nature of some of the material. However, it is the best reproduction available from the original submission.

PSU-IRL-SCI-454

Classification Numbers 1.9.2



THE PENNSYLVANIA
STATE UNIVERSITY

IONOSPHERIC RESEARCH

Scientific Report 454

THE TEMPERATURE DEPENDENCE OF THE REACTIONS OF HO_2 WITH NO AND NO_2

by

R. Simonaitis and Julian Heicklen

March 7, 1977

*The research reported in this document has been supported
by the National Aeronautics and Space Administration under
Grant No. NGL 39-009-003 and the National Science Foundation
under Grant No. GA-42856.*

IONOSPHERE RESEARCH LABORATORY



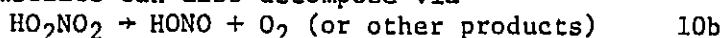
University Park, Pennsylvania



(NASA-CR-140999) THE TEMPERATURE DEPENDENCE
OF THE REACTIONS OF HO_2 WITH NO AND NO_2
(The Pennsylvania State Univ.) 43 p
42 APR 1977 AC1
CSCL 07D
32/25
Unclas
21761
N77-20179

Reaction 1b is unimportant under all of our reaction conditions. Reaction 1a was studied in competition with reaction 3 from which it was found that $k_{1a}/k_3^{1/2} = 6.4 \times 10^{-6} \exp \{-(1400+500)/RT\}$. If k_3 is taken to be $3.3 \times 10^{-12} \text{ cm}^3 \text{ sec}^{-1}$ independent of temperature, $k_{1a} = 1.2 \times 10^{-11} \exp \{-(1400+500)/RT\} \text{ cm}^3 \text{ sec}^{-1}$. Reaction 2a is negligible compared to reaction 2b under all of our reaction conditions. The ratio $k_{2b}/k_1 = 0.61 \pm 0.15$ at 245°K. Using the Arrhenius expression for k_{1a} given above leads to $k_{2b} = 4.2 \times 10^{-13} \text{ cm}^3 \text{ sec}^{-1}$ which is assumed to be independent of temperature.

The intermediate HO_2NO_2 is unstable and induces the dark oxidation of NO through reaction -2b, which was found to have a rate coefficient $k_{-2b} = 6 \times 10^{+17} \exp \{-26000/RT\} \text{ sec}^{-1}$ based on the value of k_{1a} given above. The intermediate can also decompose via



Reaction 10b is at least partially heterogeneous.

The value of k_{-2b} given above leads to the following thermal decomposition lifetimes, τ_t , at atmospheric temperature conditions:

T, °K	τ_t, S^{-1}
220	7.7×10^7
273	8×10^2
298	14.7

The above values of τ_t indicate that pernitric acid is essentially thermally stable in the lower and middle stratosphere and its formation should be considered in stratospheric models of NO_x chemistry.

NONE

PSU-IRL-SCI-454

Classification Numbers: 1.9.2

Scientific Report 454

The Temperature Dependence of the
Reactions of HO_2 with NO and NO_2

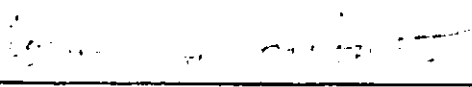
by


R. Simonaitis and Julian Heicklen

March 7, 1977

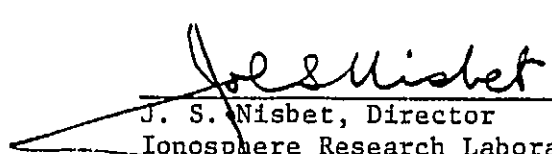
The research reported in this document has been supported by the National Aeronautics and Space Administration under Grant No. NGL 39-009-003 and the National Science Foundation under Grant No. GA-42856.

Submitted by:


Romualdas Simonaitis
Instructor in Electrical Engineering


Julian Heicklen
Professor of Chemistry

Approved by:


J. S. Nisbet, Director
Ionosphere Research Laboratory

Ionosphere Research Laboratory
The Pennsylvania State University
University Park, Pennsylvania 16802

Acknowledgment

This work was supported by the National Science Foundation through Grant No. GA-42856 and the National Aeronautics and Space Administration through Grant No. NGL-39-009-003 for which we are grateful.

Table of Contents

	<u>Page</u>
Acknowledgments	ii
Table of Contents	iii
List of Tables	iv
List of Figures	v
Abstract	vi
Introduction	1
Experimental	3
Results	4
Discussion	7
References	33

List of Tables

- Table 1: Photolysis of $\text{N}_2\text{O}-\text{H}_2-\text{O}_2-\text{NO}$ Mixtures at 213.9 nm (Low $[\text{NO}]$).
- Table 2: Photolysis of $\text{N}_2\text{O}-\text{H}_2-\text{O}_2-\text{NO}-\text{NO}_2$ Mixtures at 213.9 nm and 245°K.
- Table 3: Values of k_1/k_2' .
- Table 4: Temperature dependence of k_1/k_2' , k_{10b} and k_{-2b} .
- Table 5: Values of τ_B and k_{10b} .

List of Figures

- Fig. 1 Plots of $-\phi_i\{\text{NO}\}$ vs $[\text{NO}]/I_a^{1/2}$ in the photolysis of $\text{N}_2\text{O}-\text{H}_2-\text{O}_2-\text{NO}$ mixtures at 213.9 nm (low $[\text{NO}]$).
- Fig. 2 Typical NO decay profiles in the photolysis of $\text{N}_2\text{O}-\text{H}_2-\text{O}_2-\text{NO}$ mixtures at 213.9 nm. Run a also initially contains 7.56 mTorr of NO_2 .
- Fig. 3 Plot of $-\phi_i\{\text{NO}\}^{-1} - \beta/2$ vs $[\text{NO}_2]/[\text{NO}]$ in the photolysis of $\text{N}_2\text{O}-\text{H}_2-\text{O}_2-\text{NO}-\text{NO}_2$ mixtures at 213.9 nm and 245°K.
- Fig. 4 Plots of $\ln([\text{NO}]_i/[\text{NO}]) - ([\text{NO}]_i - [\text{NO}])/[\text{NO}_x]$ vs $f\{t\}$ in the photolysis of $\text{N}_2\text{O}-\text{H}_2-\text{O}_2-\text{NO}$ mixtures at 213.9 nm.
- Fig. 5 Plots of $\ln[1 - f\{[\text{NO}_x]\}/(C\tau_B)]$ vs t in the light-induced dark oxidation of NO.
- Fig. 6 Arrhenius plot of k_{-2b}/k_{10b} .
- Fig. 7 Arrhenius plots of k_{-2b} and k_{10b} . Closed circles assumed $E_{2b} = 0$; open circles assumed $E_{2b} = 2.5$ kcal/mole.

Abstract

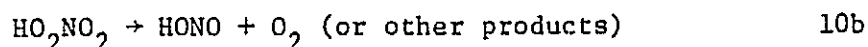
Mixtures of N_2O , H_2 , O_2 and trace amounts of NO and NO_2 were photolyzed at 213.9 nm at 245–328°K and about 1 atm total pressure (mostly H_2). HO_2 radicals are produced from the photolysis and they react as follows:



Reaction 1b is unimportant under all of our reaction conditions.

Reaction 1a was studied in competition with reaction 3 from which it was found that $k_{1a}/k_3^{1/2} = 6.4 \times 10^{-6} \exp \{-(1400 \pm 500)/RT\}$. If k_3 is taken to be $3.3 \times 10^{-12} \text{ cm}^3 \text{ sec}^{-1}$ independent of temperature, $k_{1a} = 1.2 \times 10^{-11} \exp \{-(1400 \pm 500)/RT\} \text{ cm}^3 \text{ sec}^{-1}$. Reaction 2a is negligible compared to reaction 2b under all of our reaction conditions. The ratio $k_{2b}/k_{1a} = 0.61 \pm 0.15$ at 245°K. Using the Arrhenius expression for k_{1a} given above leads to $k_{2b} = 4.2 \times 10^{-13} \text{ cm}^3 \text{ sec}^{-1}$ which is assumed to be independent of temperature.

The intermediate HO_2NO_2 is unstable and induces the dark oxidation of NO through reaction -2b, which was found to have a rate coefficient $k_{-2b} = 6 \times 10^{+17} \exp \{-26000/RT\} \text{ sec}^{-1}$ based on the value of k_{1a} given above. The intermediate can also decompose via



Reaction 10b is at least partially heterogeneous.

The value of k_{-2b} given above leads to the following thermal decomposition lifetimes, τ_t , at atmospheric temperature conditions:

$T, ^\circ K$	τ_t, s^{-1}
220	7.7×10^7
273	8×10^2
298	14.7

The above values of τ_t indicate that pernitric acid is essentially thermally stable in the lower and middle stratosphere and its formation should be considered in stratospheric models of NO_x chemistry.

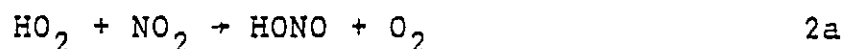
Introduction

In previous papers (1-3) we have reported on our studies of the atmospherically important reactions of HO_2 with NO and NO_2 at room temperature. By studying the chain oxidation of NO to NO_2 in the photolysis of $\text{N}_2\text{O}-\text{H}_2-\text{O}_2-\text{NO}$ mixtures at 213.9 nm and monitoring NO concentration by the chemiluminescent reaction with O_3 , the room temperature rate coefficients $k_{1a} = 1.0 \times 10^{-12} \text{ cm}^3 \text{ sec}^{-1}$ and $k_{1b} \leq 2 \times 10^{-15} \text{ cm}^3 \text{ sec}^{-1}$ were obtained (3).



This value for k_{1a} is in good agreement with our earlier (2) measurements of the lower limit and is in excellent agreement with $k_{1a} = 1.2 \times 10^{-12} \text{ cm}^3 \text{ sec}^{-1}$ determined by Cox and Derwent (4). However these values of k_{1a} are a factor of 2-3 higher than the measurements by Davis et al (5) and Hack et al (6). Our upper limit for k_{1b} is in sharp disagreement with the value of $1.4 \times 10^{-13} \text{ cm}^3 \text{ sec}^{-1}$ determined by Cox and Derwent (4) in a mixture of N_2 and O_2 (2:1) at 1 atm pressure. No other measurements of k_{1b} have been reported in the literature.

Earlier (2) we had observed that NO_2 inhibits the chain oxidation of NO and suggested the chain terminating reaction



with $k_{1a}/k_{2a} = 7 \pm 1$. Later Cox and Derwent (4) confirmed that a reaction between HO_2 and NO_2 occurs and assumed that reaction 2a was the reaction. They found $k_{2a} = 1.2 \times 10^{-13} \text{ cm}^3 \text{ sec}^{-1}$ in good agreement with our value. In our latest paper (3) we also confirmed our earlier work but in addition found that the oxidation of NO continues even after light termination. Based on this observation

the formation of pernitric acid was suggested. Thus in addition to reaction 2a the reactions



were suggested. The ratio $k_1/k_2' = 9.5 \pm 1.5$ at 25°C was obtained, where $k_2' \equiv k_2 - k_{2\text{b}}k_{-2\text{b}}/(k_{-2\text{b}} + k_{10\text{b}})$, in good agreement with our earlier work. (The reaction numbers used are the same as in our earlier paper (3) for convenience in comparing results).

In the present paper we report on our studies of the reaction of HO_2 with NO and NO_2 as a function of temperature. For the former reaction the temperature dependence of $k_{1\text{a}}$ was desired, and for the latter system it was of interest to obtain a more detailed understanding of the formation and reactions of pernitric acid, as well as to obtain the absolute values and the temperature dependence of the rate coefficients $k_{2\text{a}}$, $k_{2\text{b}}$, $k_{-2\text{b}}$ and $k_{10\text{b}}$. The method employed was the same as before (3). Briefly HO_2 radicals are generated by the photolysis of N_2O at 213.9 nm in the presence of H_2 and O_2 . In the presence of small amounts of NO and NO_2 , the reactions of interest proceed and are monitored by measuring the NO removal rate using chemiluminescent detection of NO .

Experimental

The apparatus, experimental procedure and materials were virtually identical to that described earlier (3). The only changes were to enclose the photolysis vessel in an aluminum block for precise temperature control and the volume of the vessel was changed from 2 liters to 1 liter to reduce the nonuniformity of the light distribution inside the vessel. The block could be heated with nichrome wire for temperatures above ambient or cooled by passage of nitrogen gas cooled by liquid nitrogen through a styrofoam box in which the aluminum block was enclosed. Temperatures were measured with a thermocouple and control of temperature was $\pm 1^\circ\text{C}$. The temperature of the gas inside the reaction mixture was checked by placing the thermocouple directly inside the vessel and compared to the reading outside the vessel (the normal position of the thermocouple). The two readings were identical. The light distribution inside the vessel was checked and found to be uniform within 20%.

The out-flow of the gas from the reaction vessel was always such that the total pressure during a run did not change by more than 5% and the rate of NO loss due to flow was always $< 5\%$ of the rate of loss due to photolysis.

Results

Low [NO]: The photolysis of $N_2O-H_2-O_2-NO$ mixtures at 213.9 nm and low [NO] was studied at 245, 271 and 296°K. The results are presented in Table I. At each temperature the initial quantum yield of NO disappearance, $-\phi_i\{NO\}$, is nearly proportional to $[NO]/I_a^{1/2}$ (Figure 1). Earlier more extensive data at 296°K (3) showed that $-\phi_i\{NO\}$ is proportional to $[NO]/I_a^{1/2}$ up to $\sim 14 \times 10^7 \text{ cm}^{-3/2} \text{ sec}^{-1/2}$; at higher values $-\phi_i\{NO\}$ is lower than predicted from this relationship. The present results at 296°K also show a fall off in $-\phi_i\{NO\}$ at higher $[NO]/I_a^{1/2}$ ratios, but this data is not included here. At lower temperatures the fall-off is expected to occur at a lower $[NO]/I_a^{1/2}$ ratio (see Discussion). This is apparent in the data at 245°K as can be seen in Figure 1. As the temperature decreases there is a slight but statistically significant decrease in $-\phi_i\{NO\}$ at a given $[NO]/I_a^{1/2}$ ratio.

High [NO]: In the presence of relatively high [NO] (≥ 2 mTorr) experiments were done at 245, 295, 308.5, 319 and 328°K. In some of the experiments at 245 and 295°K, NO_2 was present initially. As found before (2,3) a) the addition of NO_2 to the photolysis of $N_2O-H_2-O_2-H_2$ mixtures inhibits the conversion of NO to NO_2 , b) the oxidation shows an induction period at $T \geq 296^\circ K$ when NO_2 is present initially (see Figure 2), and c) the oxidation in the presence of NO_2 continues even after termination of the irradiation for $T \geq 295^\circ K$ (note that NO_2 is always present when the dark reaction begins, since NO_2 is a product of the light reaction). Typical curves for complete NO removal (curves b, c and d) and for a typical dark oxidation (curve a) are shown in Figure 2. No induction

periods or dark oxidation were observed at 245°K. The inhibition of NO oxidation by NO₂ is a strong function of the temperature. The effect is most pronounced at the lowest temperature and becomes progressively less important as the temperature increases. The light oxidation rates increase markedly with the temperature as can be seen from curves b, c and d of Figure 2.

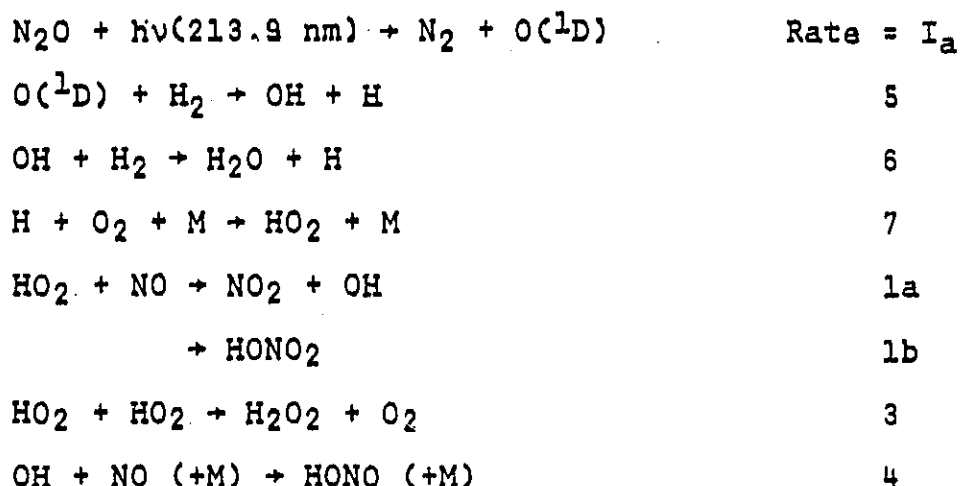
The initial experiments were done at 295°K. For the first few runs it was noted that the rate of light oxidation was much slower and the dark oxidation was small. After several runs, however, the rate became constant and the dark oxidation markedly increased. Thus unconditioned walls inhibit the oxidation.

The initial NO removal quantum yields at 245°K are presented in Table II as a function of the [NO₂]/[NO] ratio. The two sets of data presented in Table II were done in vessels of 2 and 1 liter volume, respectively, and with separately prepared mixtures of NO and NO₂. Also the 2 liter vessel was enclosed only in a styrofoam box (the aluminum block was not used). From Table II it is evident that $-\phi_i\{\text{NO}\}$ declines as the $[\text{NO}_2]_i/[\text{NO}]_i$ ratio increases. The reduction of $-\phi_i\{\text{NO}\}$ is somewhat greater for the first group than for the second. At temperatures $\geq 295^\circ\text{K}$ quantum yields were not computed, because the NO decay profiles were analyzed only in terms of the analytically integrated rate law as explained in the next section.

At temperatures $\geq 295^\circ\text{K}$ two types of experiments were done. In the first series the photolysis was carried out until complete consumption of NO occurred. In the second series of experiments irradiation was terminated before all the NO was consumed; the NO continues to be oxidized even though the irradiation has been

terminated until a limiting value of $[NO] = [NO]_{\infty}$ is reached.

Low [NO], NO₂ Absent: The photolysis of N₂O-H₂-O₂-NO mixtures at 213.9 nm may be discussed in terms of the chain mechanism given earlier (3) and using the same numbering system for the reactions:



For this system numerous other reactions are in principle possible, but they are all entirely negligible, because of the constraints imposed by relative concentrations and rate coefficients as discussed before (3).

At sufficiently low $[NO]$, reactions 1b and 4 will become negligible and chain termination by reaction 3 will predominate. For this limiting case the mechanism leads to the following rate law for NO removal:

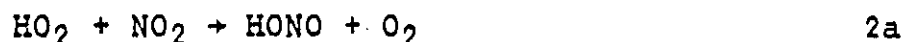
$$-\phi_1\{\text{NO}\} = k_{1a}[\text{NO}] / (k_3 I_a)^{1/2} \quad a$$

Plots of $-\phi_1\{\text{NO}\}$ vs $[\text{NO}]/I_a^{1/2}$ at 245, 271 and 296°K are shown in Figure 1. The plots at 271°K and 296°K are consistent with Eq. a. Our earlier more extensive data (3) showed that Eq. a is well obeyed up to $[\text{NO}]/I_a^{1/2} \sim 14 \times 10^7 \text{ cm}^{-3/2} \text{ sec}^{-1/2}$ at 296°K. The data at 245°K shows some fall off at higher $[\text{NO}]/I_a^{1/2}$ ratios

($> 6 \times 10^7 \text{ cm}^{-3/2} \text{ sec}^{-1/2}$), but this is expected, since at lower temperatures reaction 4 becomes more important relative to reaction 6 at lower $[\text{NO}]$, since reaction 6 has an activation energy $\sim 5 \text{ kcal/mole}$ (7). From the slopes of the plots in Figure 1 the following values of $k_{1a}/k_3^{1/2}$ ($\text{cm}^{3/2} \text{ sec}^{-1/2}$) are obtained: 7.2×10^{-7} (296°K); 5.3×10^{-7} (271°K), 4.4×10^{-7} (245°K).

The present value of $k_{1a}/k_3^{1/2}$ at 296°K is slightly higher than the value of $5.1 \times 10^{-7} \text{ cm}^{3/2} \text{ sec}^{-1}$ obtained before (3). The small difference is slightly greater than that estimated from the precision of the two studies and must be due to systematic errors. However the systematic errors should not affect the value of the activation energy difference $E_{1a} - E_3/2$, which depends on the relative change in $k_{1a}/k_3^{1/2}$ with temperature. From the present data $E_{1a} - E_3/2 = 1400 \text{ cal/mole}$ is obtained. The average value of $k_{1a}/k_3^{1/2}$ obtained before and now is $6.2 \times 10^{-7} \text{ cm}^{3/2} \text{ sec}^{-1/2}$ at 296°K . Using this average value of $k_{1a}/k_3^{1/2}$ at 296°K , the Arrhenius expression $k_{1a}/k_3^{1/2} = 6.4 \times 10^{-6} \exp\{-(1400 \pm 500)/RT\}$ is obtained. The best value of k_3 is $3.3 \times 10^{-12} \text{ cm}^3 \text{ sec}^{-1}$ at 300°K (7). Since E_3 is expected to be near zero, then $k_{1a} = 1.2 \times 10^{-11} \exp\{-(1400 \pm 500)/RT\} \text{ cm}^3 \text{ sec}^{-1}$. If the activation energy for E_3 is taken as 1000 cal/mole (7), then $k_{1a} = 2.7 \times 10^{-11} \exp\{-(1900 \pm 500)/RT\} \text{ cm}^3 \text{ sec}^{-1}$. The only other measurement of E_{1a} is by Hack et al (6). They obtained a value of $2400 \pm 300 \text{ cal/mole}$ for E_{1a} .

High $[\text{NO}]$, NO_2 Present: In order to account for 1) the inhibition of the oxidation by NO_2 , 2) the induction period in the presence of NO_2 and 3) the dark oxidation, the following reactions were proposed (3):



It was argued that pernitric acid is the responsible agent rather than the possible complex A (pernitrous acid),



because the induction period in the absence of NO_2 is very short (< 2 sec), whereas in the presence of NO_2 the induction period and the lifetime of NO in the dark oxidation are of the order of 40-60 sec. The relative importance of reactions 2a and 10b could not be determined at that time. However, in our earlier paper (2) indirect evidence for HONO formation was suggested.

The mechanism consists of reactions 1, 2, 4, 5, 6, 7 and 11, which must be introduced in the presence of NO_2 .



The chain terminating reaction, 3 is entirely negligible compared to reactions 2, 4 and 11, because of the relatively high concentrations of NO and NO_2 in these experiments. From the mechanism the following rate law during irradiation is obtained if $\beta \ll 1$

$$-\phi\{\text{NO}\} = \frac{2k_1[\text{NO}]}{k_2[\text{NO}_2] + (\beta k_{1a} + k_{1b})[\text{NO}]} [1 - k_{-2b}\alpha\tau_B(\exp\{-t/\tau_B\} - 1)] \quad b$$

where

$$\alpha \equiv k_{2b}[\text{NO}_2] / (k_2[\text{NO}_2] + (\beta k_{1a} + k_{1b})[\text{NO}])$$

and

$$\beta \equiv (k_4[\text{NO}] + k_{11}[\text{NO}_2]) / (k_6[\text{H}_2] + k_4[\text{NO}] + k_{11}[\text{NO}_2])$$

and τ_B is the lifetime of B

$$\tau_B^{-1} \equiv k_{10b} + k_{-2b} (1 - \alpha)$$

At $t = 0$ when $[B] = 0$ or when $k_{-2b} = 0$ Equation b reduces to

$$-\phi\{\text{NO}\}^{-1} - \frac{k_{1a}\beta}{2k_1} = \frac{k_{1b}}{2k_1} + \frac{k_2[\text{NO}_2]}{2k_1[\text{NO}]} \quad c$$

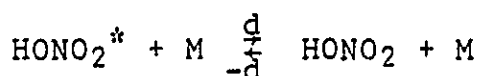
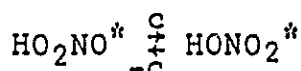
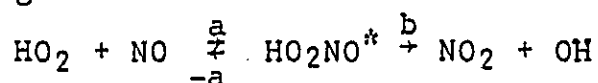
and when B is in the steady state Equation b reduces to

$$-\phi\{\text{NO}\}^{-1} - \frac{k_{1a}\beta}{2k_1} = \frac{k_{1b}}{2k_1} + \frac{k_2'[\text{NO}_2]}{2k_1[\text{NO}]} \quad d$$

where $k_2' \equiv k_2 = k_{2b}k_{-2b}/(k_{-2b} + k_{10b})$

Since $k_{1a}/k_1 \approx 1.0$ (3) a plot of $-\phi\{\text{NO}\}^{-1} - \beta/2$ vs $[\text{NO}_2]/[\text{NO}]$ should be linear after either the steady state in B is reached (Eq. d) or under conditions such that $k_{-2b} = 0$ (Eq. c). At 245°K there is no induction period for the oxidation in the presence of NO_2 and no measurable dark oxidation was observed indicating that $k_{-2b} = 0$. Thus Equation c should apply. A plot of $-\phi\{\text{NO}\}^{-1} - \beta/2$ vs $[\text{NO}_2]/[\text{NO}]$ at 245°K is shown in Figure 3 for the two sets of data given in Table II. The plot is reasonably linear for each set, but the slopes differ by about 30%. The only difference between the reaction conditions is the volume of the reaction vessel and new mixtures of NO and NO_2 were prepared for the second set. The difference in results is probably primarily due to the uncertainty in I_a , which at low temperatures had an estimated error of $\sim 15\%$ together with a lesser contribution ($\sim 10\%$) from the error in $[\text{NO}]$ and $[\text{NO}_2]$. The average value of $k_1/k_2 = 1.7 \pm 0.4$ is obtained from the slopes in Figure 3. The intercept of the plots in Figure 3 is 0.015 ± 0.005 ; therefore $k_{1b}/k_1 = 0.03 \pm 0.01$ at 245°K , and since $k_{1a} = 6.8 \times 10^{-13} \text{ cm}^3 \text{ sec}^{-1}$ at 245°K , $k_{1b} \approx (2 \pm 1) \times 10^{-14} \text{ cm}^3 \text{ sec}^{-1}$ at 245°K . Our earlier work (3) showed that $k_{1b} < (2 \pm 2) \times 10^{-15} \text{ cm}^3 \text{ sec}^{-1}$ at 295°K . Consequently if the intercept in Figure 3 is really due to reaction

1b, the rate coefficients imply that reaction 1b is still in the third order regime at 700 Torr H₂ since the activation energy is negative. Reactions 1a and 1b may be visualized as proceeding by the following mechanism



If $k_{-c} > k_d[\text{M}]$ at 700 Torr H₂ reaction 1b will be in the third order regime.

Equation d may be integrated directly, since $\beta = \text{constant}$ [note that $k_4 = k_{11}$, i.e., $k_4 = 6.0 \times 10^{-12} \text{ cm}^3 \text{ sec}^{-1}$ at $\sim 700 \text{ Torr H}_2 + (\sim 30 \text{ Torr O}_2 + \text{N}_2\text{O})$ (1,8) and $k_{11} = 8 \times 10^{-12} \text{ cm}^3 \text{ sec}^{-1}$ (7)], and if the assumption is made that $[\text{NO}]_i + [\text{NO}_2]_i = [\text{NO}] + [\text{NO}_2] \equiv [\text{NO}_x]$. The result is

$$\ln[\text{NO}]_i/[\text{NO}] - ([\text{NO}]_i - [\text{NO}])/[\text{NO}_x] = (2k_1 I_a / k_2' [\text{NO}_x]) f\{t\} \quad e$$

where

$$f\{t\} \equiv t - \frac{(\beta k_{1a} + k_{1b})}{2k_1 I_a} ([\text{NO}]_i - [\text{NO}])$$

A plot of the left-hand side of Eq. e vs $f\{t\}$ should be linear with a slope of $2k_1 I_a / k_2' [\text{NO}_x]$. Typical plots based on Eq. e at $T = 245^\circ\text{K}$, 295°K , 308.5°K , 319°K and 328°K are shown in Figure 4. It is apparent that at 245°K Equation e appears to be well obeyed, but at $\geq 295^\circ\text{K}$ the plot is nonlinear at first, but becomes linear after some time. The reason for the non-linearity initially at the higher temperatures is due to the fact that B has not yet reached the steady state. Thus at temperatures $\geq 295^\circ\text{K}$ Equation e is obeyed after some time and values of $2k_1 I_a / k_2' [\text{NO}_x]$ may be

obtained from the linear portion of the graph. At 245°K Eq. c appears to be obeyed throughout the time scale suggesting that $k_{-2b} = 0$ and thus $k_2' = k_2$, in agreement with the facts that there is no induction period for the oxidation and that there is no oxidation in the dark.

The values of k_1/k_2' obtained from the slopes of plots such as in Figure 4 are presented in Table III at the different temperatures. The average values are tabulated in Table IV. The present value of k_1/k_2' at 295°K differs significantly from the previously reported values of 7 and 9.5 at 298°K (2,3). The principle difference between the present and previous values is due to the fact that in the earlier analysis of our data the assumption was made that HO_2NO_2 was in the steady state when the values of $-\phi\{\text{NO}\}$ were determined from differential rates after the induction period. The present results analyzed in terms of the integrated rate law show that the induction period is considerably longer than appears from the NO decay profiles. Thus apparently the linearity of the plot of Eq. d at 295°K in the earlier work was fortuitous.

At 245°K the values of k_1/k_2 obtained from Eq. e are significantly higher than the value of 1.96 (lower line of Figure 3) obtained from the same runs and Eq. c. Also k_1/k_2 obtained from Eq. e appears to depend to some extent on the initial value of $[\text{NO}_2]$. This discrepancy is due to the failure of the approximation that $[\text{HO}_2\text{NO}_2] \ll [\text{NO}] + [\text{NO}_2]$ assumed in the integrated Eq. e, because at the low temperature the quantum yields for the oxidation are small. The ratio $[\text{HO}_2\text{NO}_2]/[\text{NO}_2]$ is given approximately by $k_2'[\text{NO}_2]/k_{1a}[\text{NO}]$; thus at 245°K $[\text{HO}_2\text{NO}_2]/[\text{NO}_2]$ is not negligible

since $k_2'/k_1 = 0.61$. At $\geq 295^\circ\text{K}$ $k_2'/k_1 \leq 0.036$; therefore the approximation that $[\text{HO}_2\text{NO}_2] \ll [\text{NO}] + [\text{NO}_2]$ is satisfied and Eq. e is valid. The data at 295°K in Table III supports this conclusion since k_1/k_2' appears to be independent of $[\text{NO}_2]_i$. As mentioned before it should be noted that Eq. d could not be employed at temperatures of $\geq 295^\circ\text{K}$, because initially HO_2NO_2 is not in the steady state, i.e. there is an induction period.

The value of k_1/k_2' is a strong function of the temperature. At 328°K , $k_1/k_2' = 240$; therefore $k_{2a}/k_1 \leq 4.2 \times 10^{-3}$. Since k_{2a} cannot have a negative activation energy and $E_1 = 1400$ cal/mole, then at 245°K , $k_{2a}/k_1 < 8.7 \times 10^{-3}$. At 245°K , we have already seen that $k_{-2b} = 0$, so that at 245°K , $k_2'/k_1 = k_{2b}/k_1 = 0.61 \pm 0.15$. From the value of $k_1 \approx 6.9 \times 10^{-13} \text{ cm}^3 \text{ sec}^{-1}$, we compute $k_{2b} = 4.2 \times 10^{-13} \text{ cm}^3 \text{ sec}^{-1}$, which should be independent of temperature since reaction 2b is an addition reaction of two free radicals.

Dark Oxidation: Based on the mechanism the rate of NO oxidation in the dark is described by the differential equation:

$$-d[\text{NO}]/dt = \frac{k_{-2b}k_1[\text{NO}][\text{B}]}{k_2[\text{NO}_2] + (\beta k_{1a} + k_{1b})[\text{NO}]} \quad f$$

If τ_B is constant throughout the dark period, then $[\text{B}] = [\text{B}]_0 \exp\{-t/\tau_B\}$, where $[\text{B}]_0$ is the concentration of B at $t = 0$ of the dark period. Equation f may be integrated by noting that $[\text{NO}_2] = [\text{NO}_x] - [\text{NO}]$. The result is

$$\ln([\text{NO}]_0/[\text{NO}]) - \gamma([\text{NO}]_0 - [\text{NO}])/[\text{NO}_x] = C\tau_B(1 - \exp\{-t/\tau_B\}) \quad g$$

where

$$\gamma \equiv (1 - (\beta k_{1a} + k_{1b})/k_2)$$

and

$$C \equiv k_1 k_{-2b} [\text{B}]_0 / k_2 [\text{NO}_x]$$

At $t = \infty$ Eq. g becomes

$$\ln([NO]_0/[NO]_\infty) - \gamma([NO]_0 - [NO]_\infty)/[NO_x] = C\tau_B \quad h$$

where $[NO]_\infty$ is the concentration of NO at the end of the dark run. Equation g can be rearranged to

$$\ln[1 - f([NO_x])/(C\tau_B)] = -t/\tau_B \quad i$$

where

$$f([NO_x]) \equiv \ln([NO]_0/[NO]) - \gamma([NO]_0 - [NO])/[NO_x]$$

Thus values of τ_B may be obtained from plots of the left-hand side of Eq. i vs reaction time, since the quantity $C\tau_B$ may be computed from Eq. h. Typical plots of Eq. i are shown in Figure 5 at different temperatures. The plots obey Eq. i well over most of the reaction time. Values of τ_B^{-1} obtained from the slopes of plots of Eq. i are presented in Table V.

From the definition of k_2' , and since $k_{2a} \ll k_2'$, we find that

$$k_{-2b}/k_{10b} = \frac{k_1 k_{2b}}{k_2' k_1} - 1 \quad j$$

The quantities k_1/k_2' , k_{2b} , and k_1 have already been evaluated, so that values of k_{-2b}/k_{10b} can be computed at each temperature and they are presented in Table IV. An Arrhenius plot of k_{-2b}/k_{10b} is shown in Figure 6. From the plot we find the least squares Arrhenius expression

$$k_{-2b}/k_{10b} = 3 \times 10^9 \exp\{-11500/RT\}$$

Furthermore from the definition for τ_B^{-1} , we find that

$$k_{10b} = \tau_B^{-1}/[1 + (k_{-2b}/k_{10b})(1 - \alpha)] \quad k$$

Values of k_{10b} can be evaluated for each run and they are listed in Table V. The average values of $[NO]$ and $[NO_2]$ were used to compute α and it was assumed that k_{2b} is temperature independent. From

Table V it is apparent that at 295°K $\tau_B^{-1} \approx k_{10b}$, thus the assumption that τ_B is constant throughout the dark period in the integration is valid at 295°K . However at the higher temperatures the term $k_{-2b} (1 - \alpha)$ is of the order of k_{10b} and since $\alpha \sim 1$, $k_{-2b} (1 - \alpha)$ is proportional to $[\text{NO}]/[\text{NO}_2]$. The ratio $[\text{NO}]/[\text{NO}_2]$ varies by a factor of about 2-4 from the beginning to the end of the dark period, therefore τ_B will vary by a factor of about 1.5-2. The plots of Figure 5 show very little if any curvature; therefore it would appear that the assumption $\tau_B = \text{constant}$ is justified even at $T > 295^{\circ}\text{K}$. As a further test of this assumption values of k_{10b} were also computed by using the initial values of $[\text{NO}]$ and $[\text{NO}_2]$ to compute α . The difference in the computed values of k_{10b} using the initial and average values of $[\text{NO}]$ and $[\text{NO}_2]$ was generally $< 10\%$. Finally the Arrhenius parameters for k_{-2b} and k_{10b} obtained from values of τ_B and the ratio k_{-2b}/k_{10b} as shown below lead to $A_{-2b}/A_{10b} = 6 \times 10^9$ and $E_{-2b} - E_{10b} = 11500 \text{ kcal/mole}$ in excellent agreement with the values obtained from the direct plot of k_{-2b}/k_{10b} which supports the assumption that $\tau_B = \text{constant}$ does not lead to significant error in the Arrhenius expressions for k_{-2b} and k_{10b} .

In spite of these consistency tests, there still can be considerable error in k_{-2b} and k_{10b} . Equation d, from which k_{-2b}/k_{10b} was obtained contains certain simplifications which become less and less accurate as k_{-2b}/k_{10b} becomes larger and larger, i.e. at high temperatures. Thus the values of k_{-2b} and k_{10b} at the highest temperature each could be in error by a factor of two.

The average values of k_{10b} at each temperature and the values of k_{-2b} computed from it and k_{-2b}/k_{10b} are listed in Table IV.

Arrhenius plots of k_{-2b} and k_{10b} are presented in Figure 7. The least squares Arrhenius expressions for k_{10b} and k_{-2b} are

$$k_{10b} = 1 \times 10^{(8 \pm 1)} \exp \{-14000 \pm 1500/RT\} \text{ sec}^{-1}$$

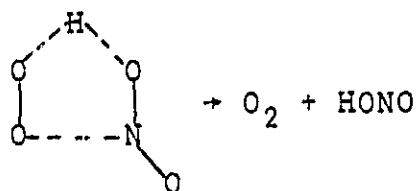
$$k_{-2b} = 6 \times 10^{(17 \pm 1.5)} \exp \{-26000/RT\} \text{ sec}^{-1}$$

In the above calculations we have assumed that reaction 2b is temperature independent since it is a radical-radical reaction. However in case there is a small temperature effect on reaction 2b we have also calculated values of k_{10b} and k_{-2b} assuming that $E_{2b} = 2.5$ kcal/mole. These values of k_{10b} and k_{-2b} are shown in Figure 6 for comparison with the values obtained for $E_{2b} = 0$. The Arrhenius expression for k_{-2b} assuming that $E_{2b} = 2.5$ kcal/mole is

$$k_{-2b} = 2.5 \times 10^{17} \exp\{-25000/RT\} \text{ sec}^{-1}$$

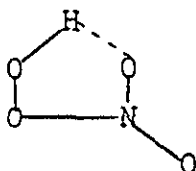
Thus k_{-2b} , A_{-2b} and E_{-2b} are not very sensitive to the value of E_{2b} . k_{10b} decreases by about a factor of 2 (somewhat less at 295°K) for a change in E_{2b} from zero to 2.5 kcal/mole. Clearly, unless E_{2b} is unusually large there is very little uncertainty introduced in the values of k_{-2b} and k_{10b} by assuming that $E_{2b} = 0$.

The value of $A_{10b} = 1 \times 10^{(8 \pm 1)} \text{ sec}^{-1}$ is too low for a homogeneous unimolecular reaction, even one proceeding through a 5 membered ring transition state such as



which would require $A \sim 10^{10} - 10^{11} \text{ sec}^{-1}$. This suggests that reaction 10b is at least partially heterogeneous, particularly at the lower temperatures. A clear indication that HO_2NO_2 can decompose

on the surface to give non-chain propagating products at 295°K is the observation that the reaction vessel had to be conditioned to give a reproducible rate of oxidation (oxidation rates for the unconditioned vessel were lower). The preexponential factors $A_{2b} = 4.2 \times 10^{-13} \text{ cm}^3 \text{ sec}^{-1}$ and $A_{-2b} = 6 \times 10^{17} \text{ sec}^{-1}$ and the activation energies $E_{2b} = 0$ and $E_{-2b} = 26 \text{ kcal/mole}$ gives $\Delta S^\circ = -49.6 \pm 10 \text{ e.u}$ and $\Delta H^\circ = 26 \text{ kcal/mole}$ for reaction 2 at 298°K. Using the following thermodynamic quantities: $S^\circ\{\text{NO}_2\} = 57 \text{ e.u}$, $S^\circ\{\text{HO}_2\} = 54.5 \text{ e.u}$, $\Delta H_f^\circ\{\text{NO}_2\} = 8.1 \text{ kcal/mole}$, $\Delta H_f^\circ\{\text{HO}_2\} = 4.9 \text{ kcal/mole}$ (9), we find $S^\circ\{\text{HO}_2\text{NO}_2\} = 62 \pm 10 \text{ e.u}$ and $\Delta H_f^\circ\{\text{HO}_2\text{NO}_2\} = -13 \text{ kcal/mole}$. Reasonably accurate values of S° and ΔH_f° for HO_2NO_2 can be estimated with the use of the partial bond method (10). Using this method we find $S^\circ\{\text{HO}_2\text{NO}_2\} = 75 \pm 2$ and $\Delta H_f^\circ\{\text{HO}_2\text{NO}_2\} = -8.5 \text{ kcal/mole}$. Clearly the value of $A_{-2b} = 6 \times 10^{17} \text{ sec}^{-1}$ is too large to be consistent with the value of $A_{2b} = 4.2 \times 10^{-13} \text{ cm}^3 \text{ sec}^{-1}$. Agreement between the entropy and enthalpy determined in this work and that calculated by the partial bond method would be obtained if $A_{-2b} \sim 1 \times 10^{15} \text{ sec}^{-1}$. Although such a low value for A_{-2b} is somewhat outside our estimated error limits, it is not impossible. In fact a reduction in E_a of 4 kcal/mole would accommodate the required factor of 600 reduction in A_{-2b} . However a high value for A_{-2b} of $\sim 10^{17} - 10^{18} \text{ sec}^{-1}$, or a low S° and high ΔH_f° for HO_2NO_2 are possible if in ground state B there is considerable restriction to internal rotation due to internal H-bond formation as represented by a structure such as



The transition state for reaction 2 can be represented by the linear structure $\text{HOO} \cdots \text{NO}_2$. Thus there may be considerable entropy of activation in going from the ground to the transition state structure leading to an abnormally high A factor for reaction -2b. On the other hand if reaction 2b really has an activation energy of 2.5 kcal/mole, then A_{2b} is 170 times larger than if $E_{2b} = 0$, and A_{2b} should be $\approx 2 \times 10^{17} \text{ sec}^{-1}$ in agreement with the calculation.

Table I

Photolysis of $\text{N}_2\text{O}-\text{H}_2-\text{O}_2-\text{NO}$ Mixtures at 213.9 nm (Low $[\text{NO}]$)^a

$10^{-7} [\text{NO}]/I_a^{1/2}$, $\text{cm}^{-3/2}\text{sec}^{-1/2}$	$10^{-13} [\text{NO}]$, cm^{-3}	$10^{-10} I_a$, $\text{cm}^{-3}\text{sec}^{-1}$	$-\phi_i\{\text{NO}\}$
T = 245°K			
1.37	0.270	3.90	6.1
2.29	0.475	4.30	10.4
2.44	0.464	3.62	13.3
4.00	0.766	3.68	18.3
5.55	1.03	3.45	22.3
11.3	2.60	5.31	32.0
11.5	1.23	1.14	39.1
12.8	2.70	4.45	49.1
T = 271°K			
2.23	0.314	1.99	16.6
5.00	0.700	1.96	22.5
8.88	1.56	3.09	43.8
12.5	1.07	0.779	70.5
13.5	1.18	0.768	71.6
T = 296°K			
3.24	0.551	2.89	31.9
4.19	0.604	2.07	33.3
6.46	0.898	1.92	43.7
10.4	0.890	0.738	71.7
15.8	1.73	1.20	79.1

a) $[\text{H}_2] = 700 \pm 30$ Torr, $[\text{O}_2] = 20-40$ Torr, $[\text{N}_2\text{O}] = 6-20$ Torr.

Table II

Photolysis of $\text{N}_2\text{O}-\text{H}_2-\text{O}_2-\text{NO}-\text{NO}_2$ Mixtures at 213.9 nm and 245°K(High $[\text{NO}]$)^a

$[\text{NO}_2]_i/[\text{NO}]_i$	$[\text{NO}]_i$, mTorr.	$[\text{NO}_2]_i$, mTorr.	$10^3 I_a$, mTorr/sec	$-\phi_i\{\text{NO}\}$
---------------------------------	-----------------------------	-------------------------------	---------------------------	------------------------

Reaction Volume = 2 liters

0	5.31	0.00	1.01	24.4
0	8.91	0.00	0.70	17.0
0.0887	4.97	0.440	1.22	13.3
0.167	5.06	0.846	1.06	11.2
0.171	4.97	0.85	1.03	9.78
0.321	5.81	1.86	0.95	5.74

Reaction Volume = 1 liter

0	4.87	0.00	2.74	29.2
0.0912	5.65	0.515	3.03	20.5
0.205	4.20	0.860	3.13	11.8
0.559	2.88	1.61	2.97	5.44
0.580	4.39	2.55	2.87	5.40

a) $[\text{H}_2] = 700 \pm 30$ Torr; $[\text{N}_2\text{O}] = 8-14$ Torr; $[\text{O}_2] = 30 \pm 5$ Torr.

Table III
Values of k_1/k_2'

$[\text{NO}]_i$, mTorr	$[\text{N}_2\text{O}]$, Torr	$[\text{NO}_2]_i$, mTorr	$10^3 I_{a,a}$, mTorr s ⁻¹	k_1/k_2'
T = 245°K				
2.88	15.6	1.61	2.97	2.36
3.92	16.3	0	3.10	3.29
4.20	15.9	0.515	3.03	2.84
4.39	15.1	2.55	2.87	2.84
4.87	14.4	0	2.73	3.72
T = 295°K				
2.60	9.73	0	1.48	16.7
4.74	8.79	0	1.37	31.1
5.21	9.10	0	1.42	31.2
5.58	8.25	2.79	1.30	32.8
6.05	8.56	0	1.36	29.9
6.32	13.0	0	2.02	16.8
6.98	8.30	1.09	1.33	24.5
7.25	7.50	4.70	1.21	20.6
7.48	7.70	4.20	1.24	33.9
T = 308.5°K				
4.74	10.6	0	3.31	61.4
8.28	10.3	0	3.33	79.6
9.58	9.26	0	3.04	69.0
9.67	11.5	0	3.76	60.9
9.86	9.26	0	3.04	79.6
11.3	11.1	0	3.64	86.9
19.7	11.2	0	3.91	93.6
22.1	15.6	0	5.30	110

Table III (Continued)

$[\text{NO}]_i$, mTorr	$[\text{N}_2\text{O}]$, Torr	$[\text{NO}_2]_i$, mTorr	$10^3 I_a^a$, mTorr s ⁻¹	k_1/k_2'
$T = 319^\circ\text{K}$				
3.82	6.22	0	2.54	78.3
7.44	9.65	0	4.04	88.5
8.60	6.77	0	2.95	119
8.98	4.05	0	1.89	136
9.26	5.29	0	2.39	123
9.26	4.16	0	1.95	121
9.86	9.02	0	3.85	112
10.0	9.1	0	3.90	171
$T = 328^\circ\text{K}$				
2.01	3.27	0	1.00	179
2.21	5.76	0	1.72	220
4.64	3.28	0	0.98	243
5.25	3.46	0	1.1	228
5.92	3.38	0	1.01	266
10.7	3.35	0	1.30	292
11.6	4.28	0	1.57	279
11.3	12.8	0	4.11	214

a) I_a corrected for NO_2 photolysis ($\leq 15\%$) with the assumption $\phi\{\text{O}(^1\text{D})\} = 1.0$ at 213.9 nm.

b) $k_2' = k_2$ at 245°K .

Table IV

Temperature dependence of k_1/k_2' , k_{10b} and k_{-2b}

$T, ^\circ K$	k_1/k_2'	k_{-2b}/k_{10b}	$10^3 k_{10b}, s^{-1}$	k_{-2b}, s^{-1}
245	1.65 ± 0.4	--	--	--
295	27.6 ± 6.2	9.27	5.33 ± 1.1	0.045
308.5	80 ± 17	26.0	11.9 ± 2.0	0.309
319	129 ± 31	39.5	29.0 ± 4.0	1.15
328	240 ± 38	70	57.6 ± 9.3	4.03

Table V
Values of τ_B and k_{10b}^a

$[\text{NO}]_i$ mTorr	$[\text{NO}]_0^b$, mTorr	$[\text{NO}_2]_i$, mTorr	$[\text{NO}_2]_0^b$, mTorr	$10^3 \tau_B^{-1}$, s^{-1}	$10^3 k_{10b}^c$, s^{-1}
T = 295°K					
6.23	3.86	--	2.37	9.20	7.25
6.51	4.12	6.79	9.18	5.87	4.88
6.51	4.55	7.56	9.52	6.30	5.04
7.63	3.81	--	3.82	5.87	4.84
10.8	7.54	--	3.26	8.40	4.63
T = 308.5°K					
3.26	2.12	--	1.14	15.0	13.0
8.65	5.81	--	2.84	16.1	9.46
8.93	5.45	--	3.48	20.0	12.7
9.49	5.59	--	3.90	15.7	10.2
19.2	12.3	--	6.90	43.3	14.2
T = 319°K					
8.02	5.07	--	2.95	68.0	32.9
8.79	5.94	--	2.85	65.6	27.1
9.26	5.46	--	3.80	48.8	25.6
9.36	6.37	--	2.99	96.5	32.9
9.36	5.45	--	3.91	63.6	32.6
9.55	5.55	--	4.00	57.1	29.3
9.74	6.19	--	3.55	50.0	22.9
T = 328°K					
2.01	1.33	--	0.68	114	89.1
4.58	2.42	--	2.16	89	52.9
5.06	2.85	--	2.21	80	47.1
5.60	2.83	--	2.77	120	67.8
11.4	6.77	--	4.63	233	62.5

a) $[\text{H}_2] = 700 \pm 30$ Torr; $[\text{O}_2] = 35 \pm 5$ Torr; $[\text{N}_2\text{O}] = 3.3 - 9.3$ Torr.

b) $[\text{NO}]_0$ and $[\text{NO}_2]$ at the beginning of the dark period.

c) Assumed $E_{2b} = 0$ in calculating k_{10b} .

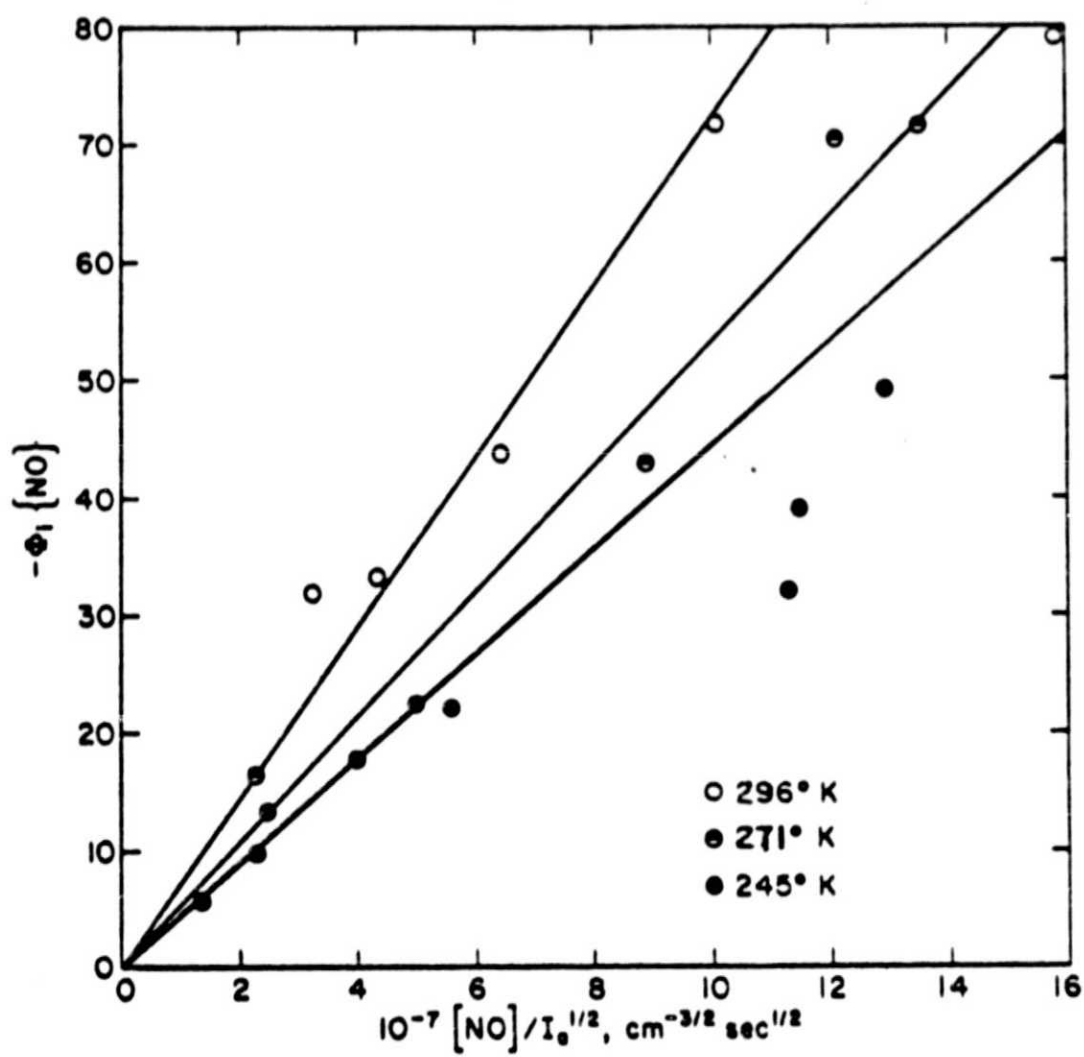


Figure 1

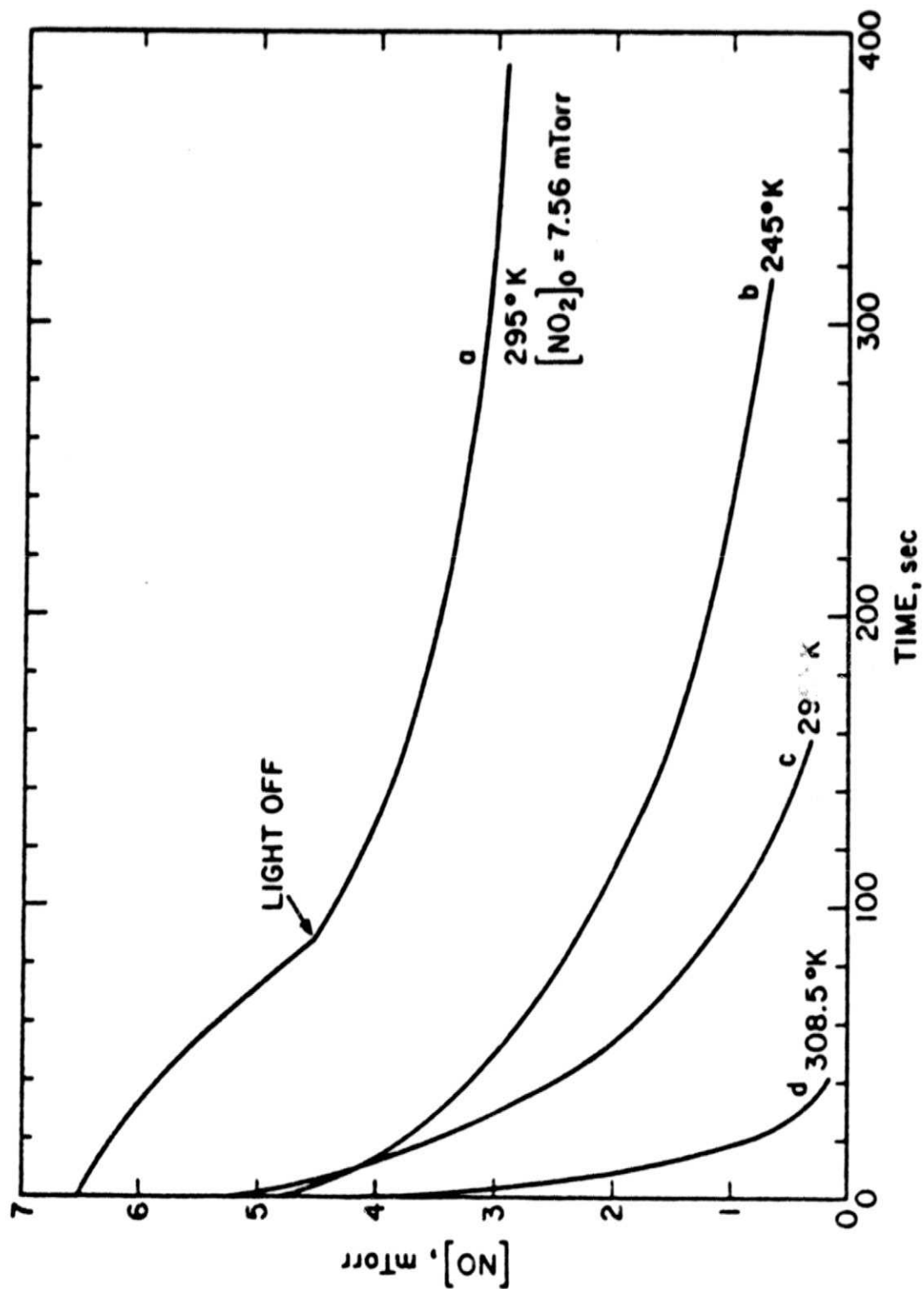


Figure 2

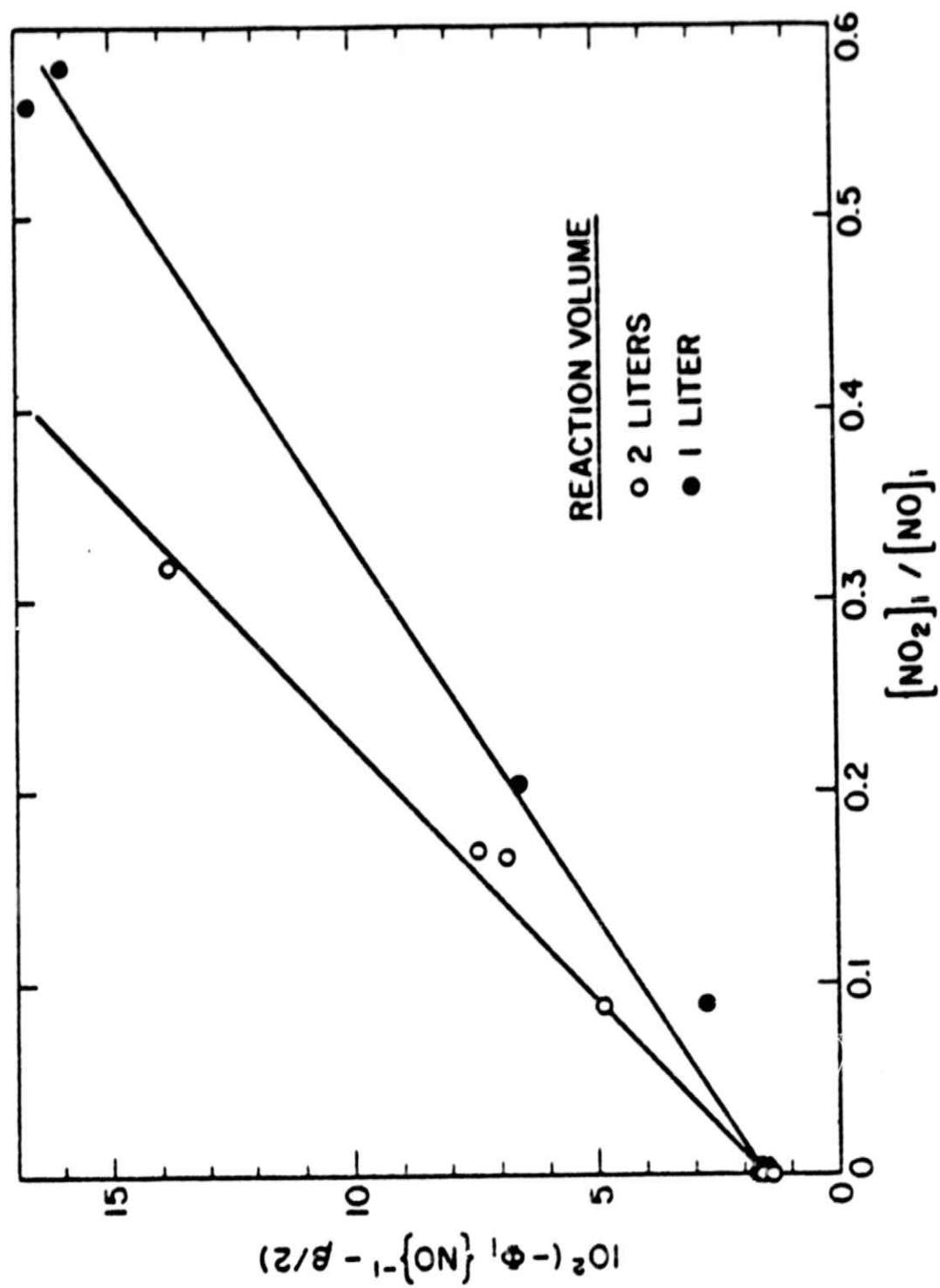


Figure 3

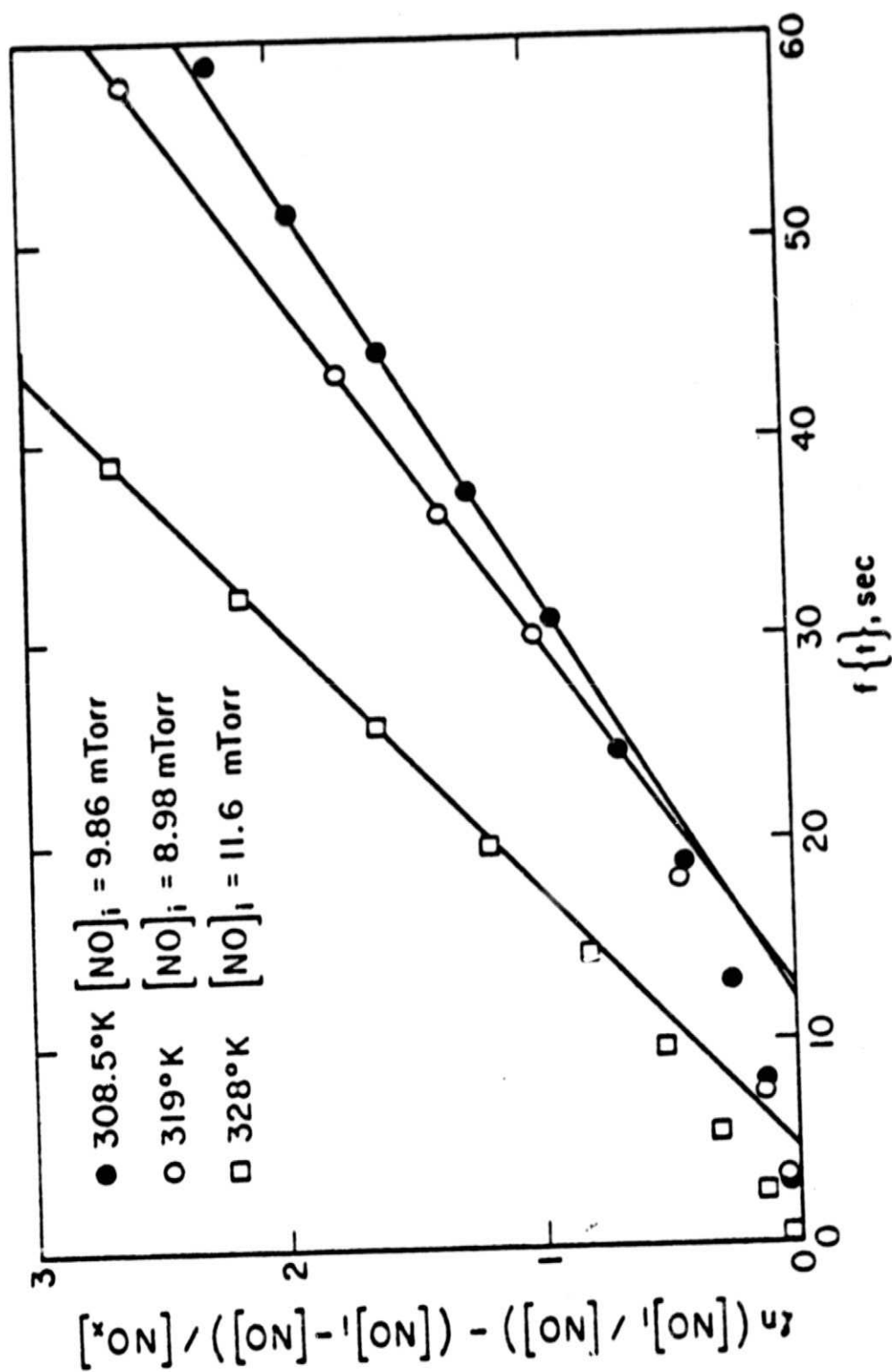


Figure 4a

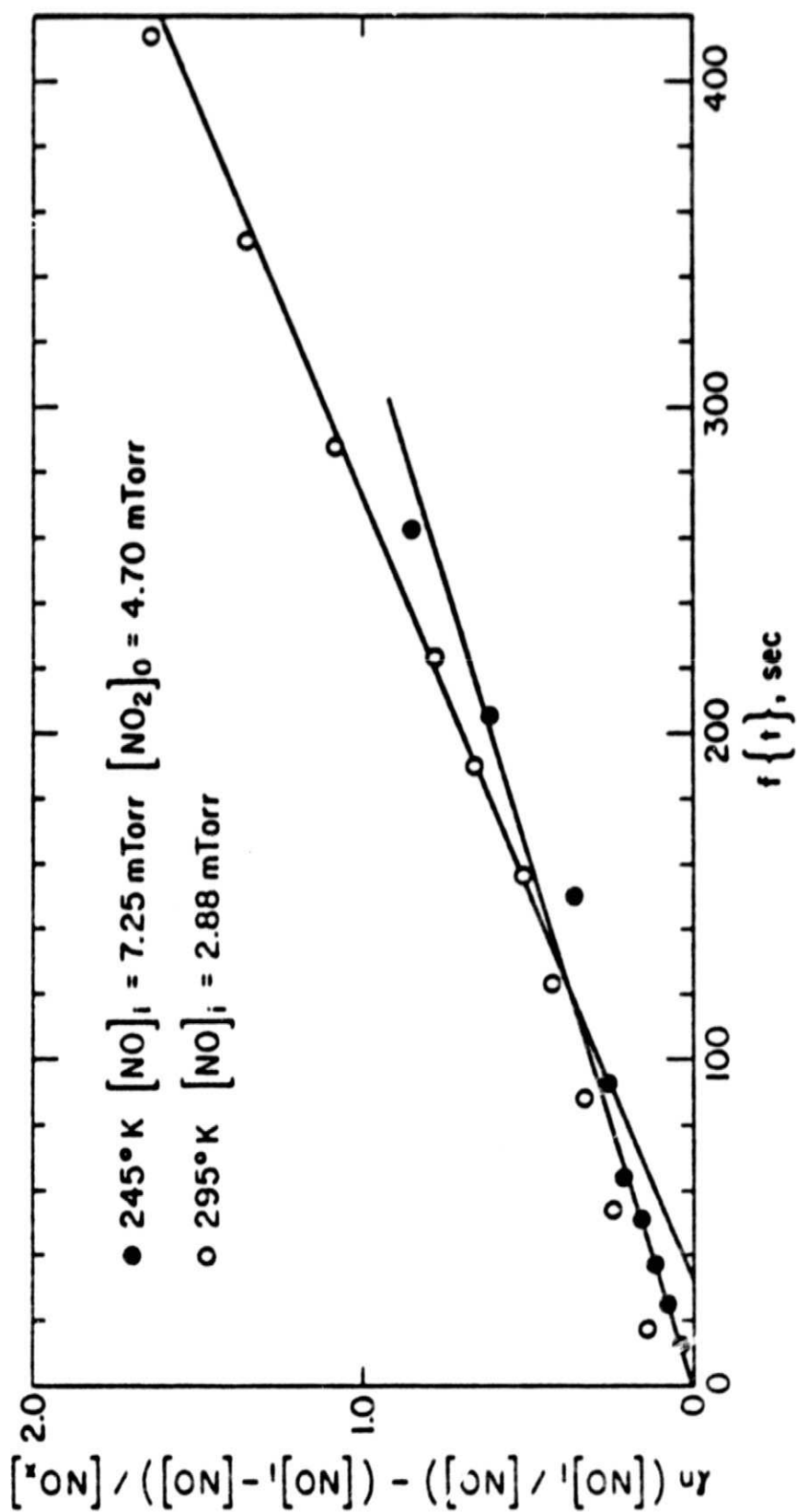


Figure 4b

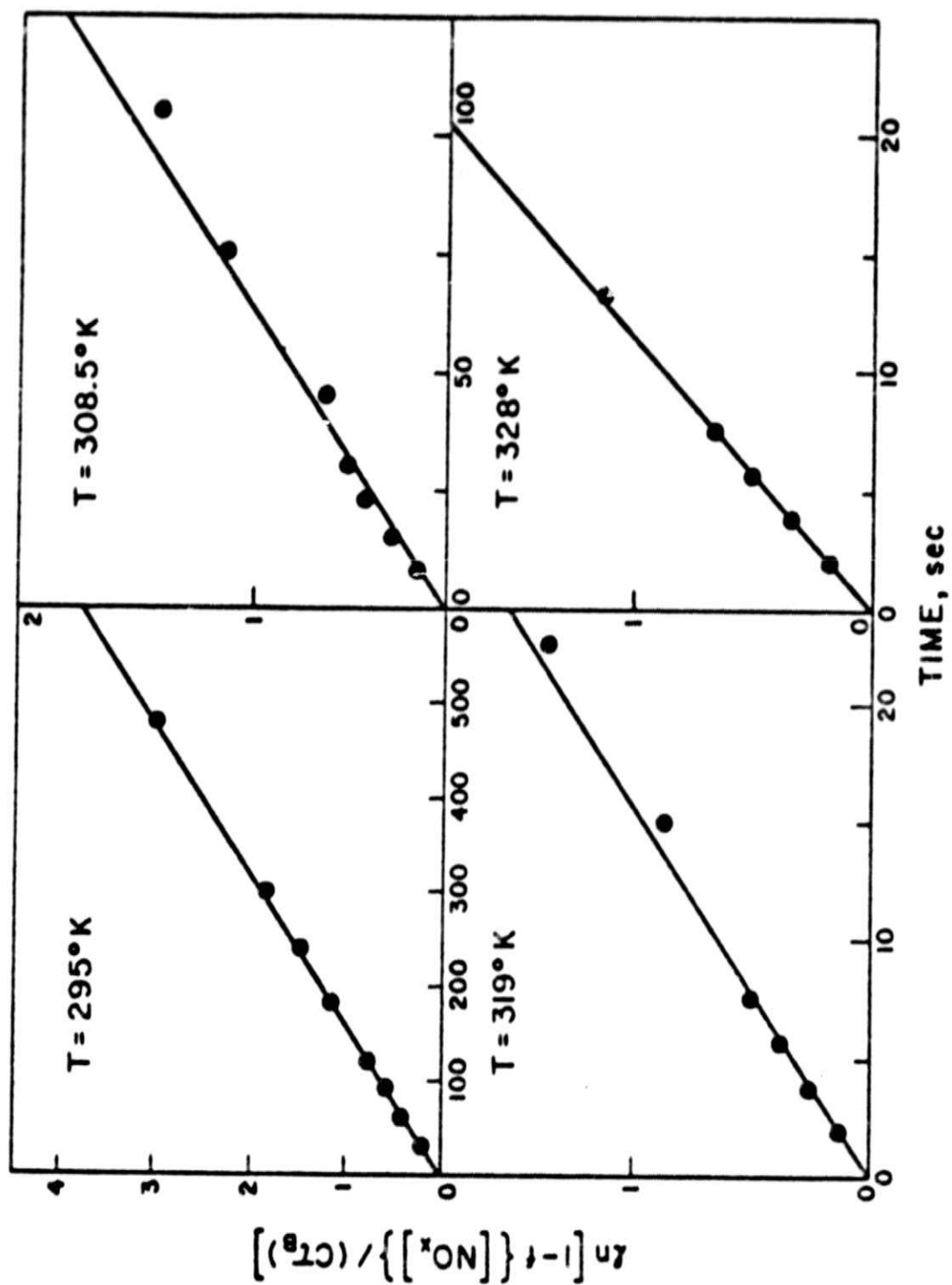


Figure 5

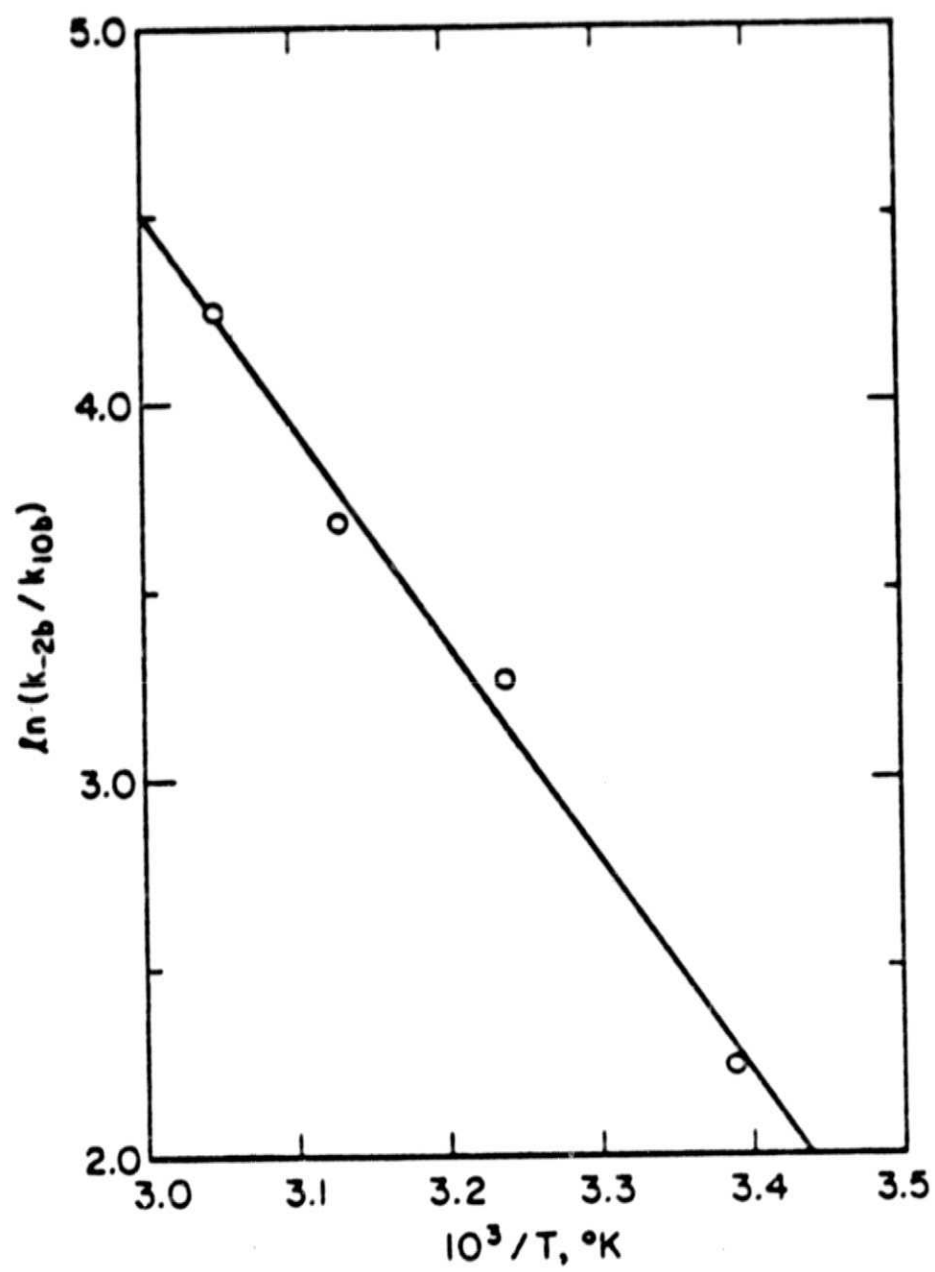


Figure 6

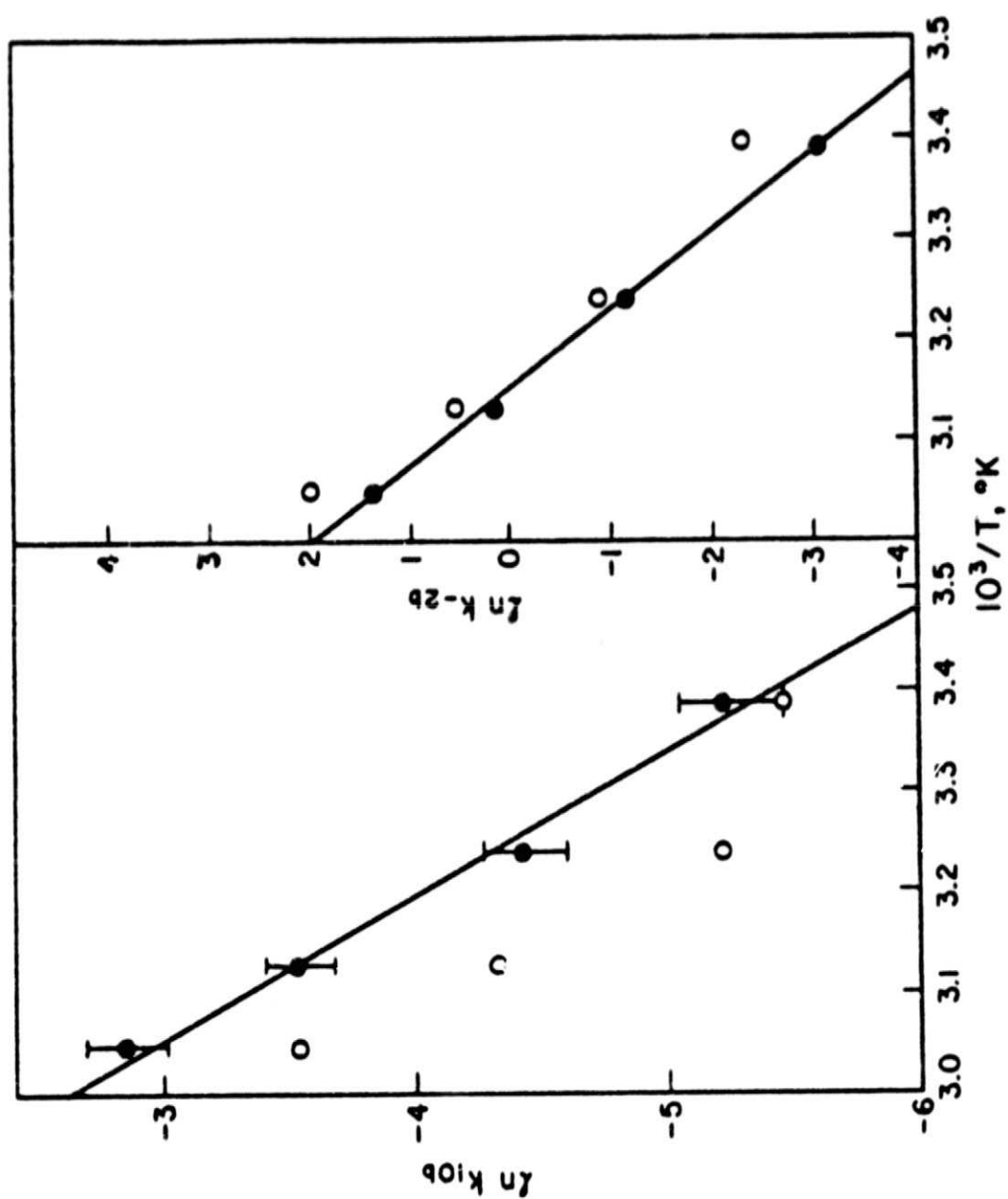


Figure 7

References

1. R. Simonaitis and J. Heicklen, J. Phys. Chem., 77, 1096 (1973).
2. R. Simonaitis and J. Heicklen, J. Phys. Chem., 78, 653 (1974).
3. R. Simonaitis and J. Heicklen, J. Phys. Chem., 80, 1 (1976).
4. R. A. Cox and R. G. Derwent, J. Photochem., 4, 139 (1975).
5. D. D. Davis, W. A. Payne, and L. J. Stief, Science, 179, 280 (1973); W. A. Payne, L. J. Stief, and D. D. Davis, J. Am. Chem. Soc., 95, 7614 (1973).
6. W. Hack, K. Hoyer mann and H. G. Wagner, Intern. J. Chem. Kinetics, Symposium No 1, 329 (1975).
7. R. F. Hampson, Jr. and D. Garvin, National Bureau of Standards Technical Note 866, "Chemical Kinetic and Photochemical Data for Modelling Atmospheric Chemistry" (1975).
8. R. Overend, G. Paraskevopoulos and C. Black, J. Chem. Phys., in press (1976).
9. J. G. Calvert and J. N. Pitts, Jr., "Photochemistry", Wiley and Sons, p. 815 (1967).
10. S. W. Benson, "Foundations of Chemical Kinetics", McGraw-Hill Inc., p. 665 (1960).